Electronic Supplementary Material (ESI) for Nanoscale Horizons.

# Supporting Information

## Ultratough and ultrastrong graphene oxide hybrid films *via* a polycationitrile approach

*Jian Chang, Miao Zhang,* Qiang Zhao, Liangti Qu,* Jiayin Yuan**

J. Chang, Dr. M. Zhang, Prof. J. Yuan
Department of Materials and Environmental Chemistry, Stockholm University, 10691 Stockholm, Sweden.
E-mail: miao.zhang@mmk.su.se; jiayin.yuan@mmk.su.se

Prof. Q. Zhao
Key Laboratory of Material Chemistry for Energy Conversion and Storage (Ministry of Education), School of Chemistry and Chemical Engineering, Huazhong University of Science and Technology, Luoyu Road No. 1037, Wuhan 430074, China

Prof. L. Qu
Department of Chemistry, & Department of Mechanical Engineering, Tsinghua University, Beijing, 100084, China
E-mail: lqu@mail.tsinghua.edu.cn

## Chemicals and characterizations

**Chemicals and materials.** Graphite powder (325 mesh) was obtained from Tsinghua University (Beijing, China). 2,2'-Azobis(2-methylpropionitrile) (AIBN), 2,6-di-*tert*-butyl-4-methylphenol (DBMP), potassium permanganate, 4-vinylbenzyl chloride (VBCl) and hydrogen peroxide (30% in water) were purchased from Sigma-Aldrich. 2,2'-Azobis[N-(2-hydroxyethyl)-2-methylpropionamide] (VA86) was purchased from FUJIFILM Wako Chemicals Europe GmbH. 1-Cyanomethylimidazole (CMIm) was purchased from AstaTech, Inc. Diethyl ether (>99.8%) was purchased from Honeywell Corporation. Sulphuric acid (95%), ethanol, methanol and acetone were purchased from VWR International Ltd. Hydrochloric acid (37%) and ammonium hydroxide were purchased from Fisher Chemical. Methyl sulfoxide-$d_6$ for nuclear magnetic resonance (NMR) measurements was purchased from Acros Organics. Poly(vinylidene fluoride) (PVDF) hydrophilic membrane (diameter = 47 mm, pore size = 0.22 μm) was purchased from Merck Millipore. All the chemicals were of analytical grade without further purification. Deionized water purified by a Milli-Q system was used in all experiments.

**Characterizations.**

Proton Nuclear Magnetic Resonance ($^1$H NMR) spectra were recorded on Bruker Avance III 400MHz.

Gel permeation chromatography (GPC) was performed using NOVEMA Max linear XL columns with a mixture of 80% of aqueous acetate buffer and 20% of methanol. Conditions: flow rate 1.00 mL min$^{-1}$, PSS polymer standards using RI detector-Optilab-DSP-Interferometric Refractometer (Wyatt-Technology).

X-ray photoelectron spectroscopy (XPS) analysis of GO films and GO based nanohybrids was carried out by Thermo Escalab 250XI under ultrahigh vacuum conditions in the range of ~ $10^{-10}$ mbar by using a monochromatic Al Kα X-ray source ($h\nu$ = 1486.6 eV) operated at 150 W.

Fourier transform infrared (FTIR) spectroscopy was performed on IR spectrometer (670-IR). Background and sample scan times were set to 16 and samples were gently ground in a mortar prior to the measurement.

X-ray diffraction (XRD) test was performed on a Panalytic X'Pert Pro (Malvern Panalytical, Malvern, UK) utilizing non-monochromatic Cu K$\alpha$ radiation. An acceleration voltage of 40 kV, current of 40 mA and step-size of 0.033° were used for each analysis and data was collected from 5° to 40°.

Scanning electron microscopy (SEM) was performed on a JSM-7000F microscope (Tokyo, Japan). Samples were attached onto an aluminum substrate using double-sided carbon adhesive tape, and were imaged and analyzed at 15 kV. Non-conducting samples were sputtered with gold before characterization.

Atomic force microscopy (AFM) was performed on Multimode AFM (Veeco Metrology) for the characterization of the thickness of GO nanosheets that were deposited on mica surface and surface morphologies of GO film and GO based nanohybrids.

Mechanical tests: All the specimens for mechanical tests were cut into rectangular strips with a width of 3 mm and lengths of 30 mm by a razor blade. Mechanical tensile tests were conducted on an Instron 5960 universal testing machine (Instron, USA). The thickness of the specimens was obtained by measuring the cross-section of the stripped specimens by SEM. Tensile strength and failure strain were recorded when the fracture occurred, Young's modulus was calculated from the slope of the linear region of the stress-strain curves and fracture toughness is calculated by integrating the areas under the stress-strain curves. All the reported data were the average of over 4 strips of the same samples.

**Synthesis of 1-cyanomethyl-3-(4-vinylbenzyl)imidazolium chloride (IL1) monomer.** 1-Cyanomethylimidazole (CMIm) (11 g, 0.10 mol) accompanied with a stabilizer, 2,6-di-*tert*-butyl-4-methylphenol (DBMP) (50 mg, 0.23 mmol) was dissolved in 15 ml MeOH. Then, 4-vinylbenzyl chloride (VBCl) (15.3 g, 0.10 mol) was added slowly into solution at room temperature. The reaction was stirred at room temperature for one hour and then at 40°C for 12 h. The oily precipitate was washed with 3 x 500 ml diethyl ether before vacuum-dried into a solid at 40°C for 12 h. (Yield: 91%)

**Synthesis of poly(1-cyanomethyl-3-(4-vinylbenzyl)imidazolium chloride) (PIL1).** IL1 monomer (20 g) and the VA86 initiator (200 mg, 1 wt%) were dissolved in a degassed aqueous solution (200 ml) under nitrogen. The reaction mixture was stirred, heated to and kept at 70°C for 24 h under nitrogen atmosphere. Afterwards, the solution was dropped into excessive acetone (500 mL) and the obtained precipitates were filtered off, washed with acetone for 3 times and vacuum-dried at 50°C for 12 hours. (Yield: 48%)

**Synthesis of 1-methyl-3-(4-vinylbenzyl)imidazolium chloride (IL2) monomer.** A mixture of 1-methylimidazole (MIm) (30 g, 0.35 mol) and 30 ml MeOH was added into a 500 mL round-bottom flask, accompanied with 2,6-di-*tert*-butyl-4-methylphenol (DBMP) (100 mg, 0.45 mol) as the stabilizer. Then, 4-vinylbenzyl chloride (VBCl) (50.80 g, 0.33 mol) was slowly added into the solution. The reaction was stirred at room temperature for one hour and then increased to and kept at 40 °C for 12h. After that, the precipitate was obtained by washing with diethyl ether for three times and dried by high vacuum. (Yield: 90%)

**Synthesis of poly(1-methyl-3-(4-vinylbenzyl)imidazolium chloride) (PIL2).** IL3 monomer (20 g) and the AIBN initiator (200mg, 1 wt%) were dissolved in degassed DMSO (200 ml) under nitrogen. The reaction mixture was stirred, heated to and kept at 70°C for 24h under nitrogen atmosphere. Afterwards, the solution was dropped into excessive acetone (500 mL) and the obtained precipitate was filtered off, washed with acetone for 3 times and vacuum-dried at 50°C for 12 hours. (Yield: 47%)

**Preparation of GO.** Graphite powder (1g, 325 mesh) was added slowly into 95% sulphuric acid (30 ml) into a 250 ml flask. The reaction slurry was vigorously stirred at 20°C for 30 min. Potassium permanganate (3.0 g) was added slowly into the slurry *via* further stirring for over 10 min and the oxidation reaction was performed for more than 3h at 20°C. Then the reaction was terminated by pouring the reaction system into 500 ml deionized water at 20°C, and 10 ml $H_2O_2$ aqueous solution (30 wt %) was slowly added to reduce Mn(VII) species. Graphite oxide (GO) was obtained by separation from the reaction system *via* centrifugation at 10 000 rpm for 40 min. The obtained GO was washed with 1 000 mL aqueous HCl solution (v/v= 1/10 from 37% concentrated aqueous HCl solution and deionized water) for 3 times *via* centrifugation at 10 000 rpm for 50 min. After washing with deionized water for 3 times, GO dispersion was exfoliated by mild sonication (input energy < 30 J $L^{-1}s^{-1}$) at 20°C for 10 min. Afterwards, the GO dispersion was performed to another 3 cycles of centrifugation at 3000 rpm (30 min for each) to remove the graphite powder and unexfoliated GO agglomerates. Finally, the dilute GO dispersion was concentrated again by centrifugation at 10 000 rpm for 50 min, which generates the GO stock.

As a control experiment, conventional synthesis of GO based on the Charpy-Hummers oxidation method was also conducted. Briefly, graphite powder (1 g, 325 mesh) was added to a 250 mL flask, followed by the slow addition of 95% sulfuric acid (30 mL). After vigorously stirring at 20°C for 30 min, the reaction system was mixed with potassium permanganate (3.0 g) by further stirring for another 10 min. The first oxidation was performed over 1 h under 35°C and the following second oxidation was initiated by the addition of 30 mL $H_2O$ in 10 min, and kept at

95°C for 15 min. After that, the reaction was terminated and collected by the same method at room temperature by preparation of GO as mentioned above.

**Preparation of GO with different sizes.** Briefly, GO nanosheets of different sizes were obtained *via* a two-step centrifugation approach. Initially, the GO dispersion was centrifuged at 8000 rpm for 40 min, to separate the supernatant from the precipitate. The supernatant contains smaller GO (sGO), and the precipitate was collected and redispersed *via* sonication for a second centrifugation step at 4000 rpm for 40 min. The produced supernatant in the second centrifugation step was labeled as middle-sized GO (mGO), and the residue precipitate as large-sized GO (lGO). Here, we utilized SEM images to measure the size distributions of sGO, mGO and lGO. The obtained mean area (and the standard deviation) of GO sheets was calculated from their sizes.

**Preparation of the GO hybrid film (GO/PIL1-*x*%-NH$_3$).** The GO stock was diluted by deionized water and treated by 10 min mild sonication plus 10 min stirring. PIL1 was dissolved in deionized water at a defined concentration. Then, a defined amount of PIL1 aqueous solution (the mass of PIL1 is 1.0-5.0 wt% relative to GO) was added dropwise into the GO dispersion and stirred for 1 h followed by sonication for 10 min to obtain a homogeneous dispersion. After homogenization, the obtained dispersion was vacuum-filtered off into a hybrid film termed GO/PIL1-***x***% (***x***=1 to 5, ***x***% denotes the relative amount of PIL1 to GO) on a PVDF filtration support, dried at room temperature for 24 h (22°C). Finally, the GO/PIL1-***x***% film together with the underlying PVDF filter support was annealed in an NH$_3$-rich atmosphere (0.2 bar NH$_3$ vapor pressure) in equilibrium with an aqueous NH$_3$ solution (25 wt%) for 24h at 20°C in a closed chamber. The obtained film termed "GO/PIL1-***x***%-NH$_3$" was then dried in air till constant weight. A free-standing GO/PIL1-***x***%-NH$_3$ was easily peeled off from the PVDF filter support.

**Preparation of the GO hybrid film (GO/PIL1-3%-NH$_3$) with different thickness.** To prepare GO/PIL1-3%-NH$_3$ with different thickness, the GO stock was diluted into 6 mg/ml GO dispersion by deionized water, then a defined amount of PIL1 aqueous solution (the mass of PIL1 is 3 wt% relative to GO) was added dropwise into the 6 mg/ml GO dispersion of 3 ml, 5 ml and 10 ml in volume, respectively. After homogenization, the obtained dispersions were vacuum-filtered off into hybrid films of different thickness. The obtained films were treated by NH$_3$ vapor for crosslinking. The thickness of these films was measured by cross-sectional SEM images.

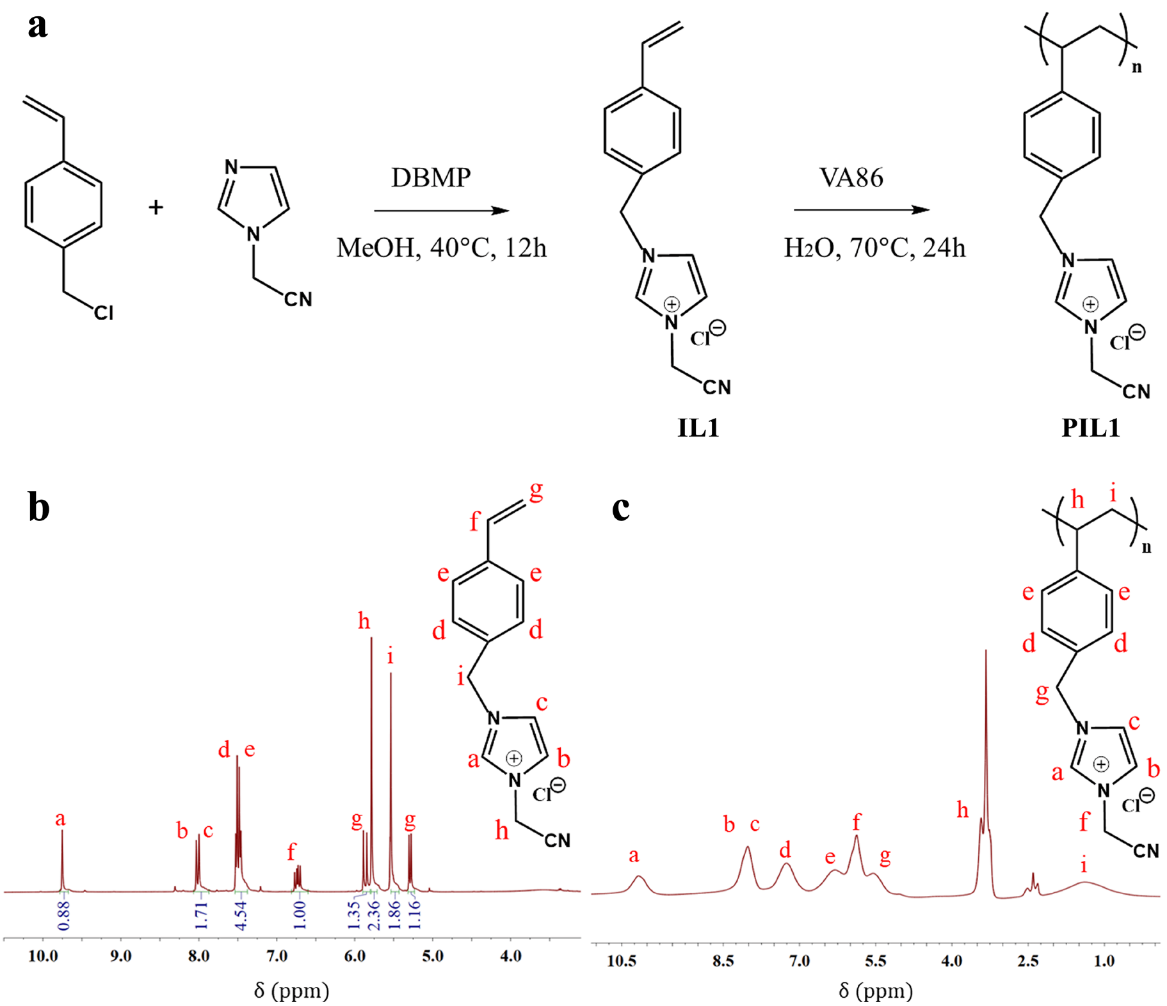

**Figure S1.** (a) Schematic synthesis of monomer IL1, and its polymer PIL1 by radical polymerization. (b, c) $^1$H NMR spectra of IL1 and PIL1, respectively, in DMSO-$d_6$.

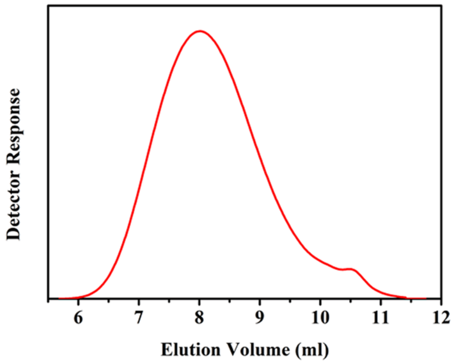

**Figure S2.** GPC trace of PIL1. The apparent number- and weight-averaged molecular weight is $M_n$=7.01×$10^4$ g/mol and $M_w$=6.71×$10^5$ g/mol, respectively. PDI=9.6.

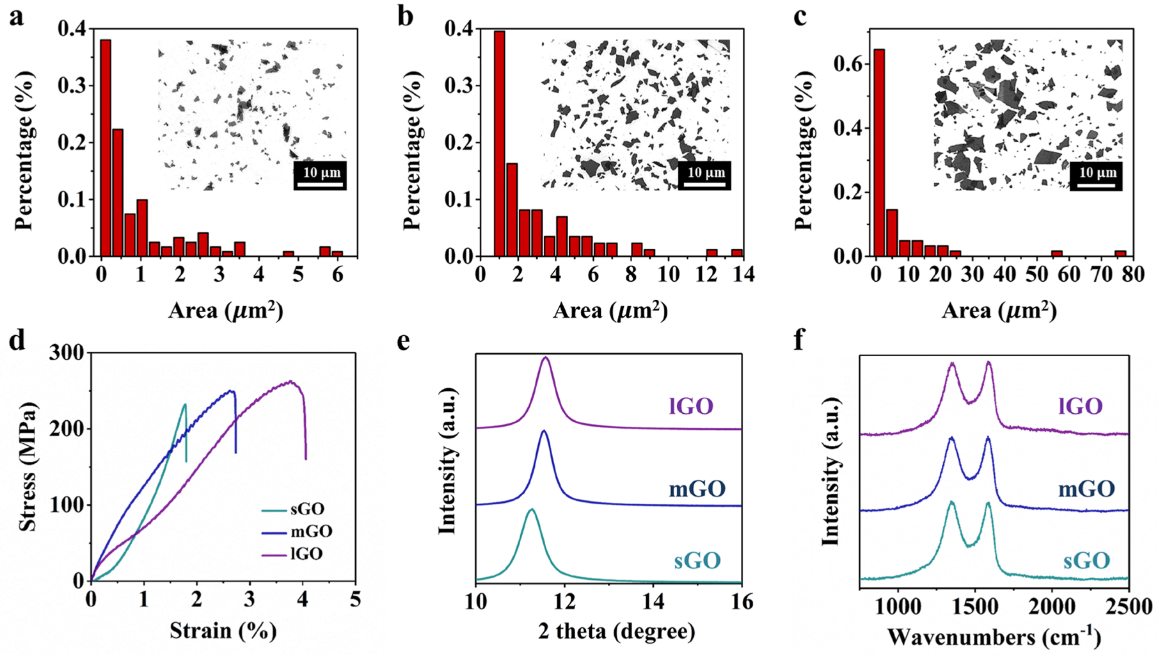

**Figure S3.** Area distributions of GO sheets of different size groups: small-sized GO (sGO)(a), middle-sized GO (mGO)(b) and large-sized GO (lGO)(c). The insets are their representative SEM images. The mean area values of sGO, mGO, and lGO are statistically calculated to be 1.05 ± 1.24, 3.09 ± 2.57, and 10.33 ± 26.43 μm$^2$, respectively. Tensile stress-strain curves (d) and XRD patterns (e) of sGO, mGO, and L-GO films. Their interlayer spacing is 7.85, 7.67, and 7.64 Å for sGO, mGO and lGO films, respectively. Films prepared by larger GO sheets have a more compact and aligned layered structure than those with smaller sheets. The larger GO sheets with less oxygenated functional groups could construct less hydrogen bonding with water, resulting in a smaller interlayer spacing while sGO with a higher fraction of oxygenated functionality groups can accommodate the water molecules *via* hydrogen bonding to broaden GO interlayer.[1] As a result, there is drastic enhancement in Young's modulus, tensile strength, strain and toughness of GO films with increasing GO size from sGO, mGO to lGO, as shown in Figure S3d and Table S1. (f) Raman spectra of sGO, mGO, and lGO films. The peak intensity ratio of the D band (~1350 cm$^{-1}$) to the G band (~1585 cm$^{-1}$) ($I_D/I_G$) is calculated to indicate structure defects in GO sheets. $I_D/I_G$ of sGO, mGO and lGO is 1.02, 1.00 and 0.98, which means fewer defects in the larger GO sheets. Owing to a more compact layered structure and fewer defects, lGO are advantageous over sGO in fabricating GO or GO hybrid films of high mechanical performance.

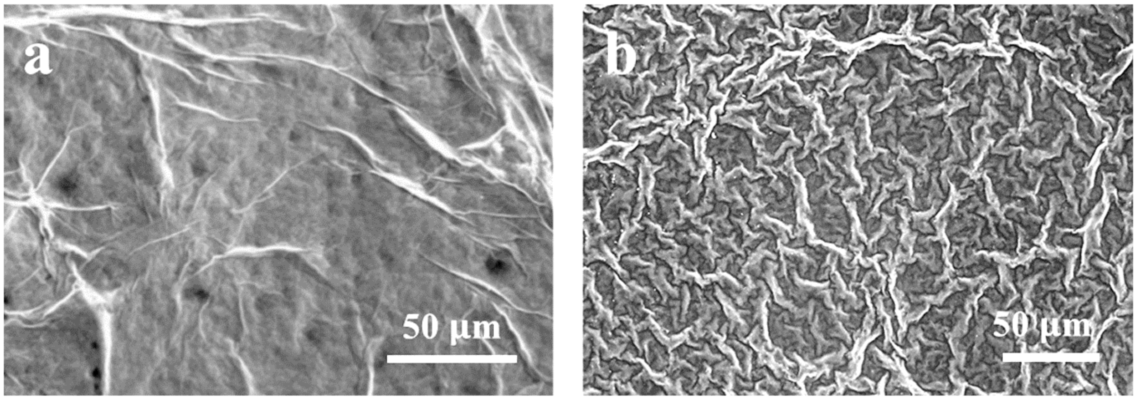

**Figure S4.** SEM surface morphologies of the GO film (a) and GO/PIL1-3%-NH3 (b).

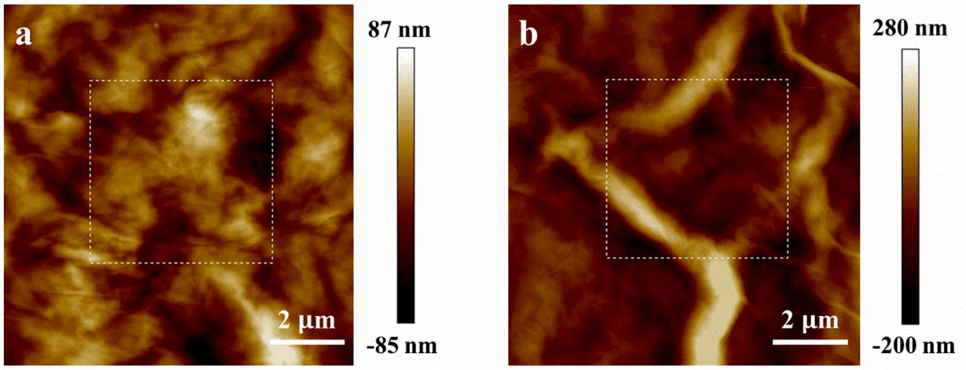

**Figure S5.** AFM images of the GO film (a) and GO/PIL1-3%-NH3 (b), showing an average roughness of 18±2 nm, and 53±12 nm within 5 × 5 μm$^2$, respectively. The insets in Figure (a) and (b) show two examples with a roughness of 20 nm, and 66 nm, respectively.

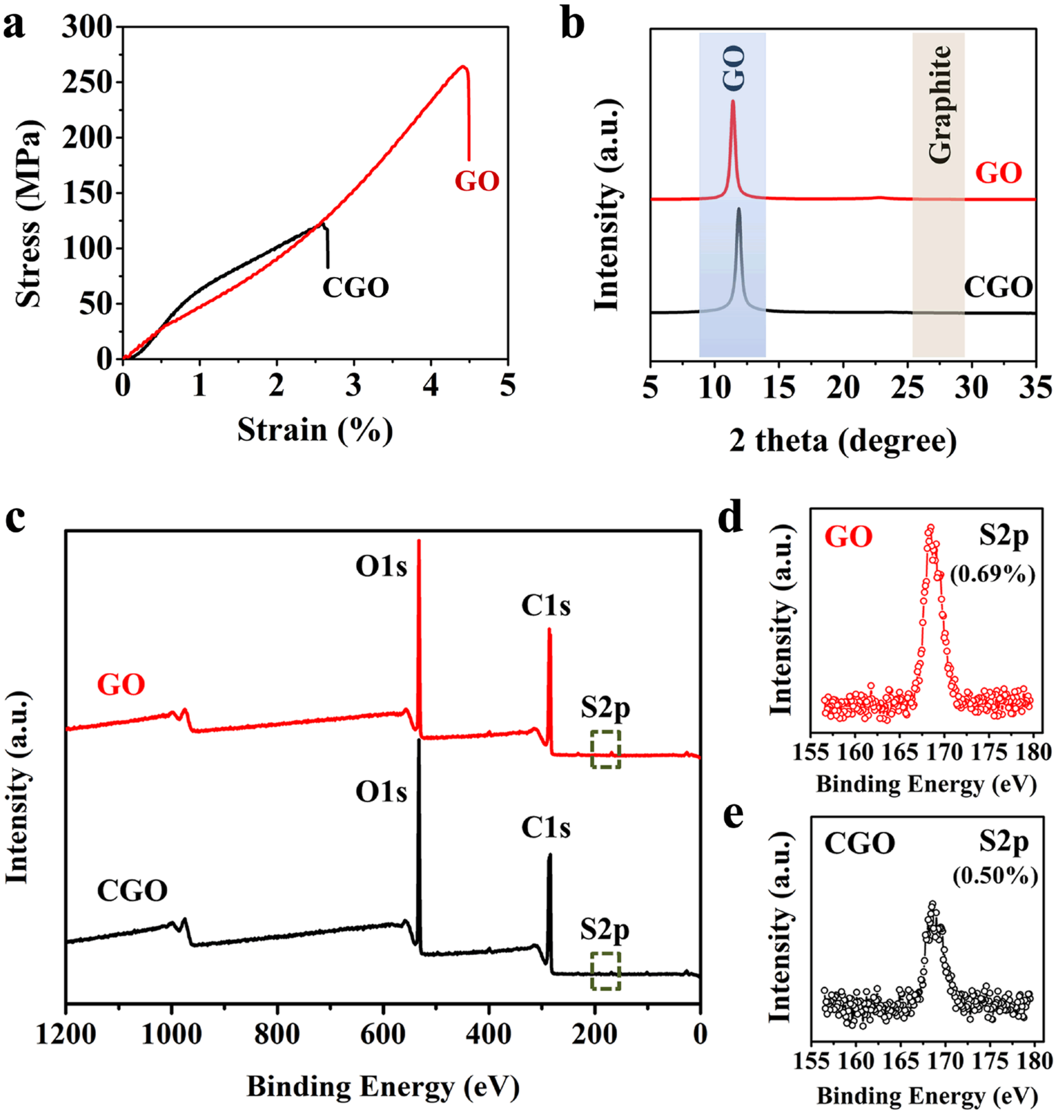

**Figure S6.** (a) Tensile stress-strain curves of conventional GO (**CGO**) film prepared from GO nanosheets synthesized *via* classic Hummer's method (black curve) and our GO film *via* room temperature oxidation method (red curve). (b) XRD patterns of our GO film and **CGO** film, showing the complete removal of the graphite phase. (c) XPS spectra of the GO film and **CGO** film. The C/O atomic ratio of GO film and CGO film are 2.45 and 2.32, respectively, obtained by the atomic % results from XPS survey. The GO film possesses a higher C/O atomic ratio than the CGO film, reflecting a lower oxygen-functionality content. S2p spectra of the GO film (d) and **CGO** film (e). The larger interlayer spacing of the GO film results from a higher content of the organosulfate species (0.69 at.%) than the conventional one (0.50 at.%).

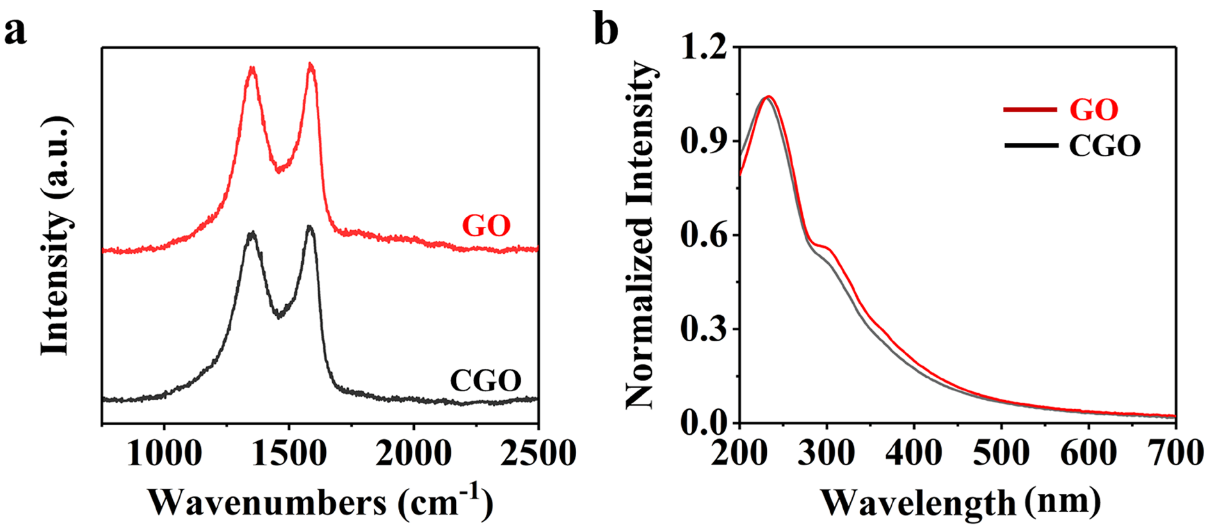

**Figure S7.** (a) Raman spectra of conventional GO (CGO) film *via* classic Hummer's method and our GO film *via* room temperature oxidation. There is no significant difference on their $I_D/I_G$ ratios despite of repeated tests, which is possible due to their similar skeleton structure and types of functional groups. (b) UV-Vis absorption spectra of GO and CGO films. Both spectra show a maximum absorbance peak at ~230 nm, corresponding to conjugated ketones or dienes.[2] In parallel, the absorption of GO is stronger than that of CGO in the visible region associated with the graphitic domains.[3] Therefore, GO sheets synthesized at lower temperature (20 ℃) possess larger graphitic domains than CGO due to the lower extent of carbon atom rupture during room temperature oxidization.[4] UV-Vis absorption spectra provides clear evidence that room-temperature oxidization of graphene can effectively produce high quality GO with less structure defects and larger graphitic domains, leading to stronger inter-sheet interactions between GO sheets.

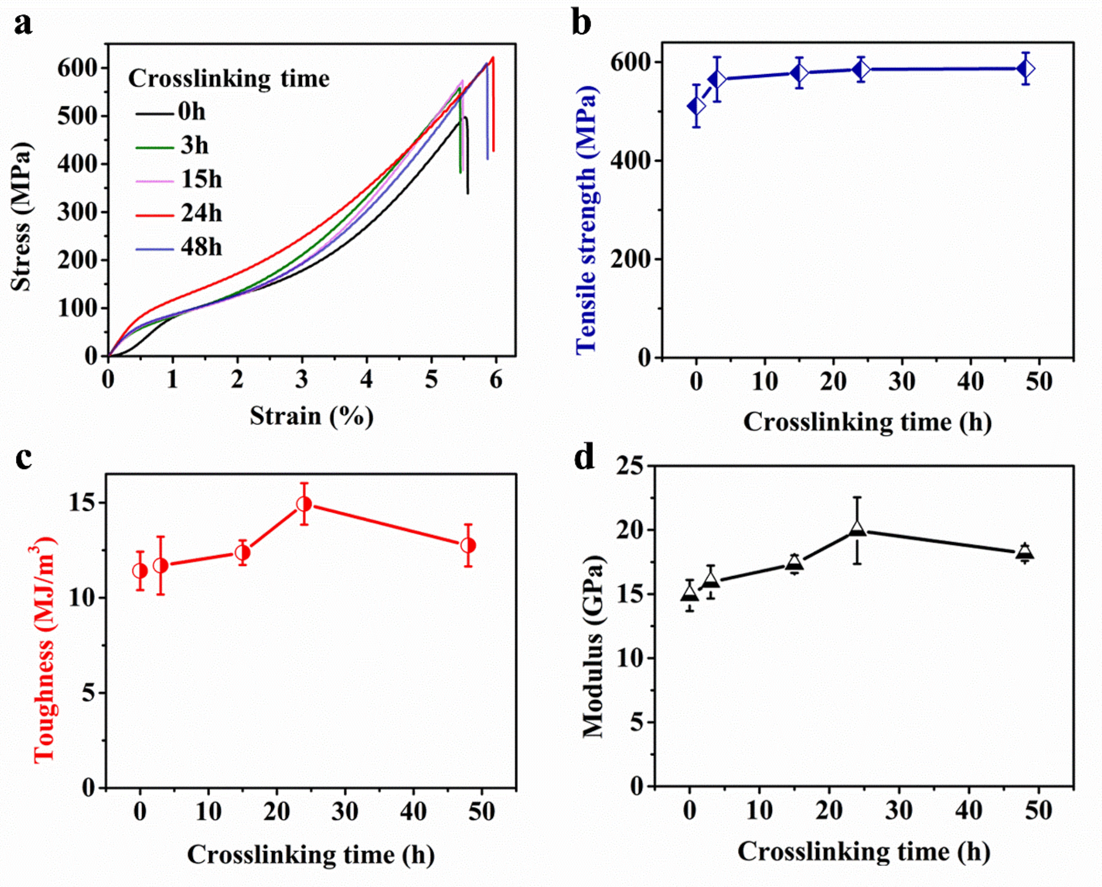

**Figure S8.** (a) Tensile stress-strain plots of GO/PIL1-3%-$NH_3$ at different exposure time (0, 3, 15, 24 and 48h) to $NH_3$ vapor. The plots of tensile strength (b), toughness (c) and modulus (d) of GO/PIL1-3%-$NH_3$ *vs.* exposure time (0, 3, 15, 24 and 48h) to $NH_3$ vapor.

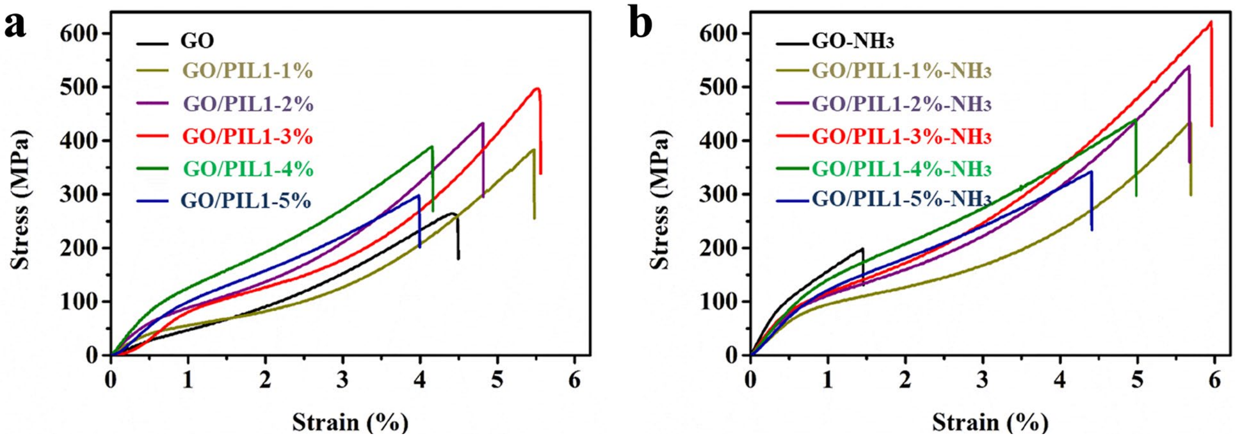

**Figure S9.** Tensile stress-strain curves of GO film and GO/PIL1-***x***%, ***x***=1 to 5 (a), and their $NH_3$-treated samples GO-$NH_3$ and GO/PIL1-***x***%-$NH_3$ (***x***=1 to 5) (b).

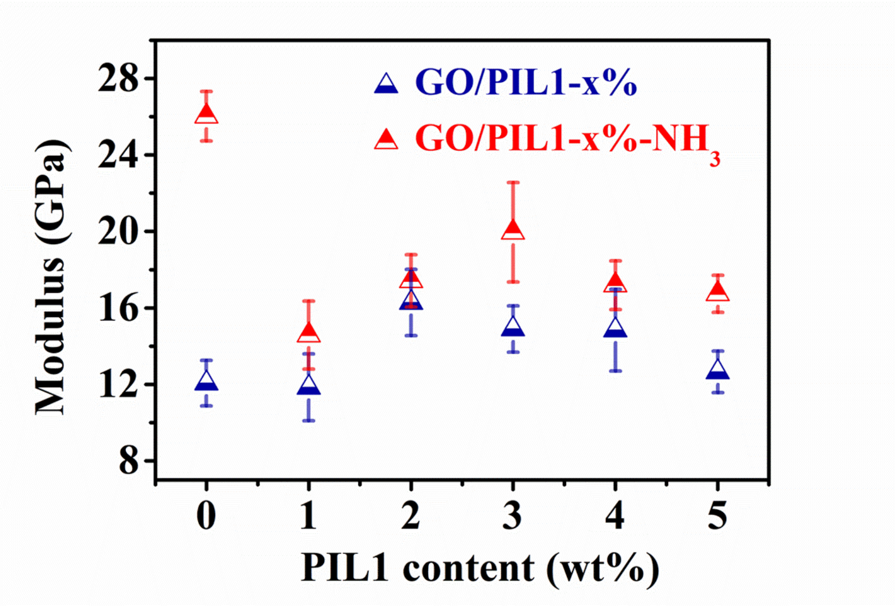

**Figure S10.** The comparisons of Young's modulus of GO/PIL1-***x***% and GO/PIL1-***x***%-$NH_3$ with different PIL1 content (***x***=0 to 5). When ***x***=0, GO/PIL1-0% is the pure GO film and GO/PIL1-0%-$NH_3$ is the pure GO film after $NH_3$ treatment.

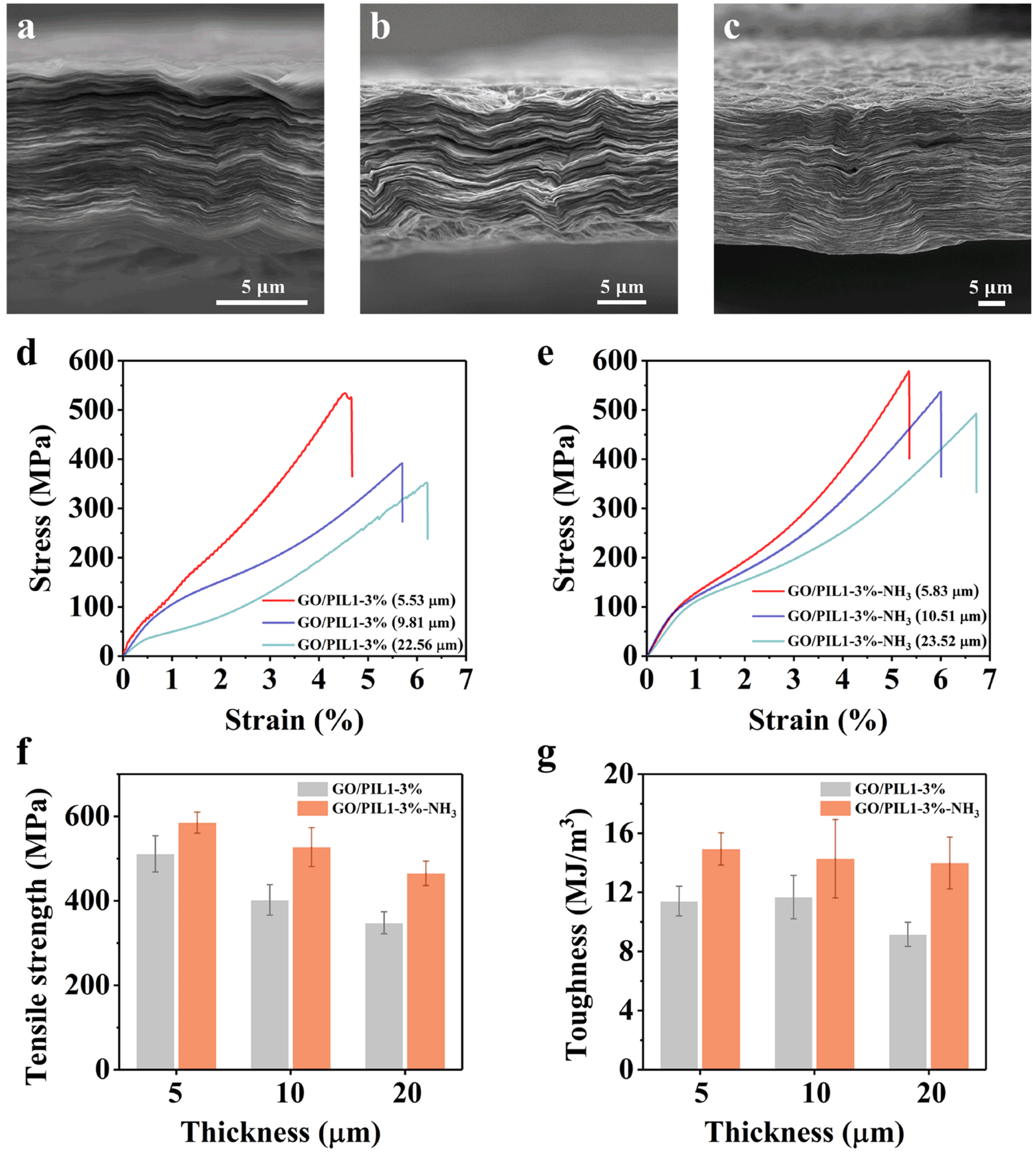

**Figure S11.** The SEM images of the cross-section of GO/PIL1-3%-$NH_3$ with the thickness of 5.83 ± 0.21 μm (a), 10.51 ± 0.55 μm (b) and 23.52 ± 0.79 μm (c). Tensile stress-strain curves of GO/PIL1-3% (d) and GO/PIL1-3%-$NH_3$ (e) with different thicknesses. The comparisons of tensile strength (f) and toughness (g) between GO/PIL1-3% and GO/PIL1-3%-$NH_3$ with different thicknesses.

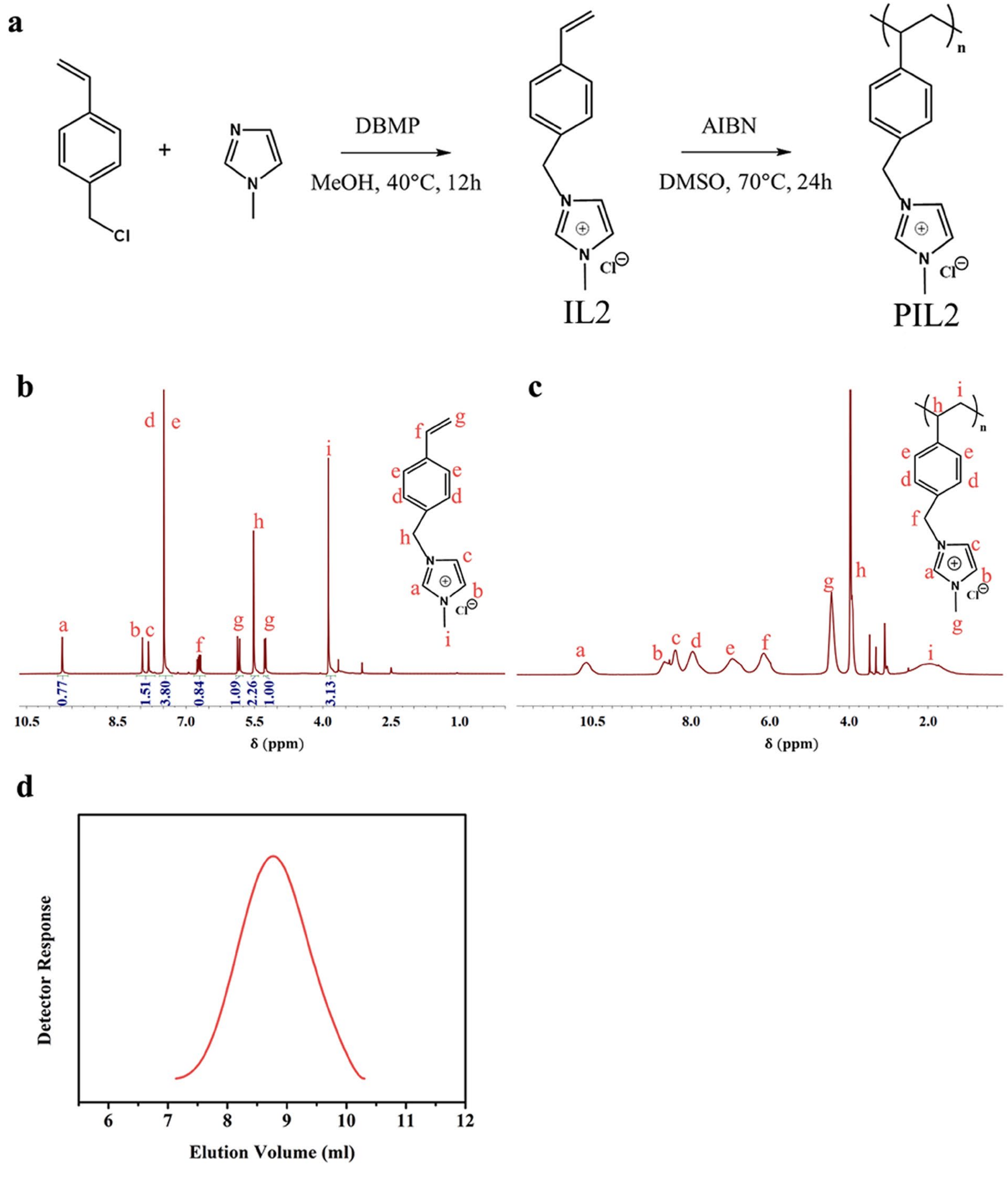

**Figure S12.** (a) Schematic synthesis of monomer IL2 and polymer PIL2 by radical polymerization. (b, c) $^1$H NMR spectra of IL2 and PIL2, respectively, in DMSO-$d_6$. (d) GPC trace for PIL2. apparent $M_n$=1.03×10$^5$ g/mol; apparent $M_w$=2.05×10$^5$ g/mol; DPI=2.0.

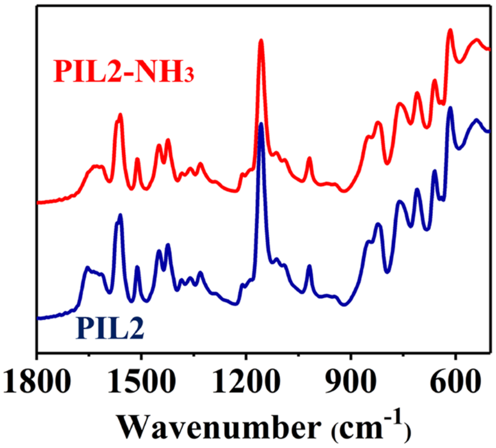

**Figure S13.** FT-IR spectra of PIL2 and its NH$_3$-treated sample PIL2-NH$_3$. Both are similar.

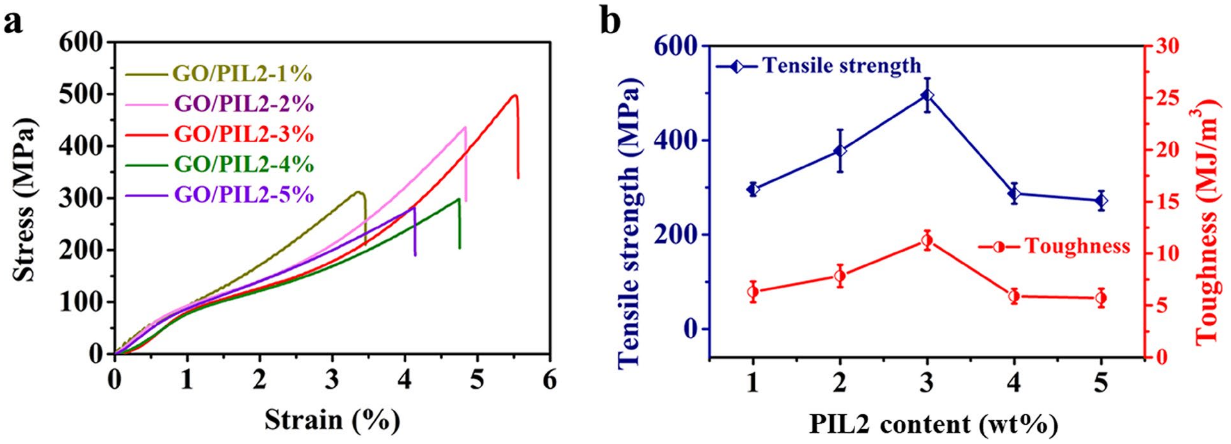

**Figure S14.** (a) Tensile stress-strain curves of GO/PIL2-***x***% with the different amount of PIL2 relative to GO (***x***=1 to 5). (b) The plots of tensile strength and toughness of GO/PIL2-***x***% (***x***=1 to 5) *vs.* the PIL2 content.

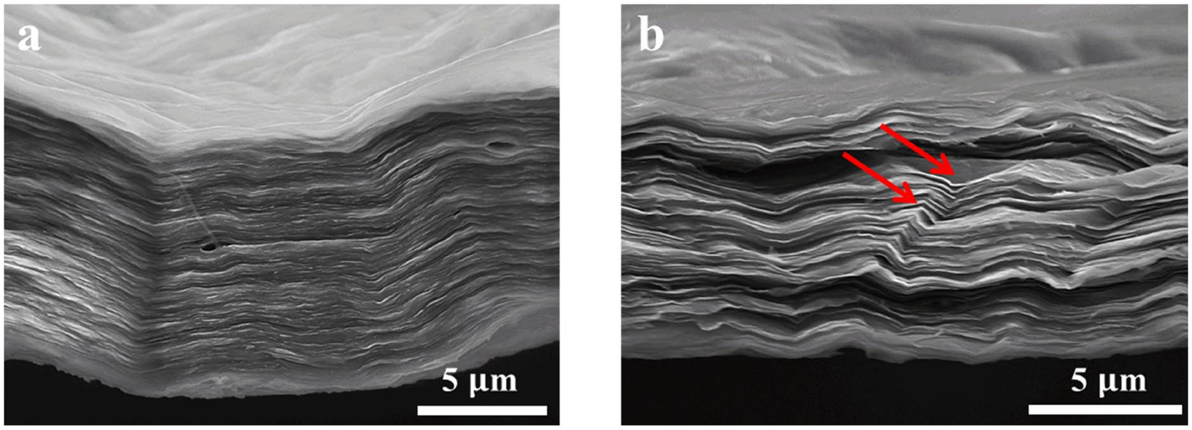

**Figure S15.** SEM cross-sectional images of GO/PIL1-3%-$NH_3$ between vertical shear (a) and horizontal fracture (b). Horizontal fracture in (b) causes pulling-out effect of individual GO sheets (red arrows) while cross-section of GO/PIL1-3%-$NH_3$ is relatively flat and smooth upon vertical shear in (a).

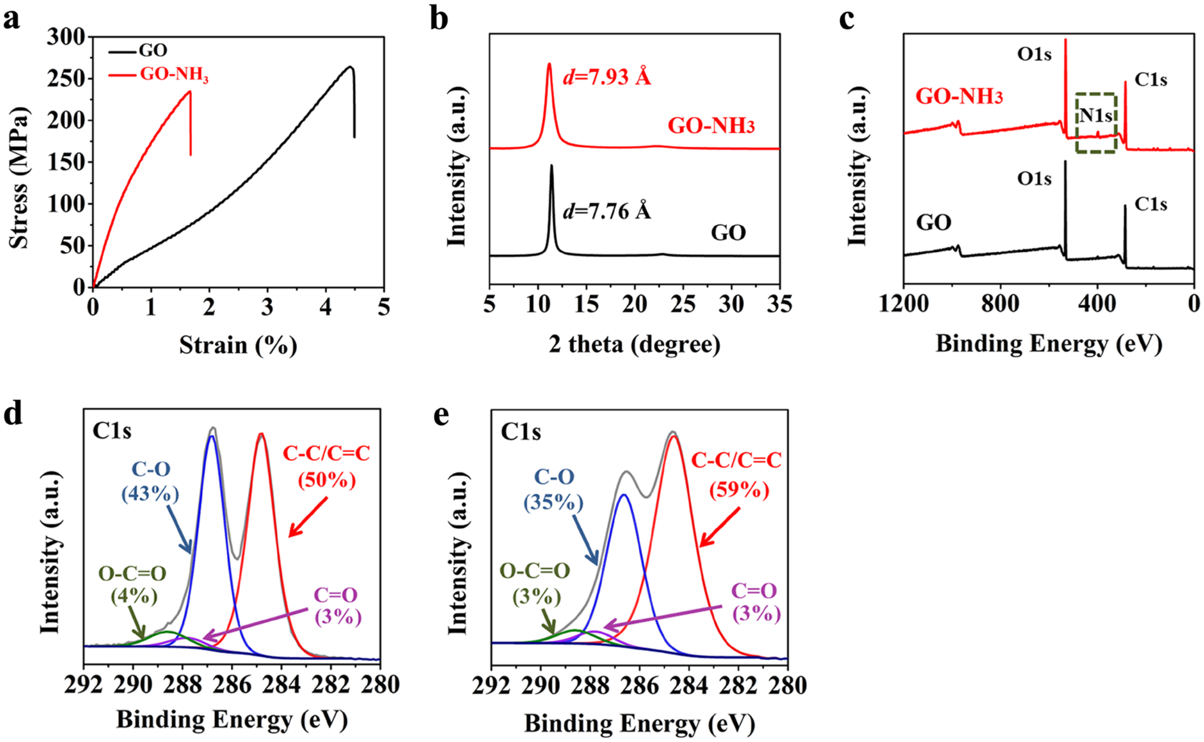

**Figure S16.** (a) Tensile stress-strain curves of the pristine GO film (black line) and the GO film after $NH_3$ vapor treatment (GO-$NH_3$) (red line). (b) XRD patterns of the GO film and GO-$NH_3$ film. The calculated interlayer spacing *d* of the GO film and GO-$NH_3$ film is 7.76 Å and 7.93 Å, respectively. (c) XPS spectra of the GO film and GO-$NH_3$ film. The nitrogen content of GO-$NH_3$

film is 4.04 at%. The high resolution spectrum of C 1s of GO film (d) and GO-$NH_3$ film (e). The content of C-O is decreased in GO-$NH_3$ film because of the reaction between ammonia and GO nanosheets (ammonia reacts with carboxylic acid group and the epoxide group).

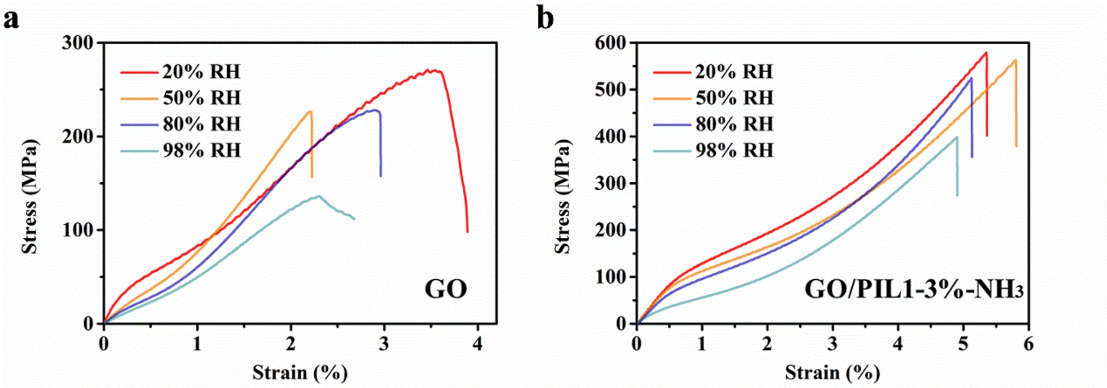

**Figure S17.** Typical tensile stress-strain curves of GO film (a) and GO/PIL1-3%-$NH_3$ (b) under different environmental relative humidity (RH) of 20%, 50%, 80% and 98%, respectively.

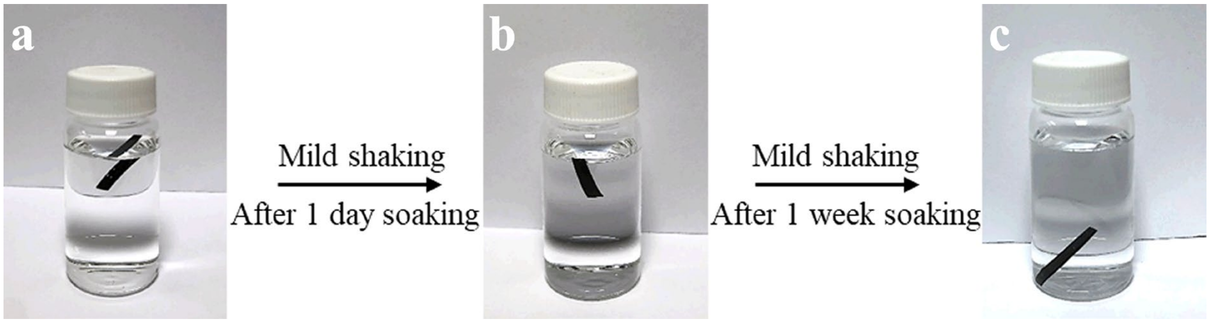

**Figure S18.** Photographs of GO/PIL1-3%-$NH_3$ before (a) and after soaking in water for one day (b), and then one week (c), followed by mild shaking.

**Table S1.** The mechanical property data of sGO, mGO, and lGO films.

| Sample | Thickness (μm) | Strength (MPa) | Strain (%) | Toughness ($MJ/m^3$) | Modulus (GPa) |
|---|---|---|---|---|---|
| sGO | 5.36±0.32 | 217±21 | 1.73±0.33 | 1.31±0.17 | 10.30±0.43 |
| mGO | 5.45±0.43 | 241±22 | 2.87±0.61 | 3.90±1.23 | 11.72±2.06 |

| | | | | | |
|---|---|---|---|---|---|
| lGO | 5.21±0.16 | 253±16 | 4.06±0.12 | 5.19±0.43 | 12.06±1.19 |

**Table S2.** The *d*-spacing of conventional GO (CGO) synthesized by Hummers method, our synthesized GO film, GO/PIL1-1%-$NH_3$, GO/PIL1-2%-$NH_3$, GO/PIL1-3%-$NH_3$, GO/PIL1-4%-$NH_3$ and GO/PIL1-5%-$NH_3$.

| Sample | Angle (°) | Interlayer spacing (Å) |
|---|---|---|
| CGO (Hummers method) | 11.87 | 7.45 |
| GO | 11.41 | 7.76 |
| GO/PIL1-1%-$NH_3$ | 11.31 | 7.83 |
| GO/PIL1-2%-$NH_3$ | 11.27 | 7.85 |
| GO/PIL1-3%-$NH_3$ | 11.17 | 7.92 |
| GO/PIL1-4%-$NH_3$ | 11.05 | 8.01 |
| GO/PIL1-5%-$NH_3$ | 10.94 | 8.09 |

**Table S3.** The mechanical property data of conventional GO (CGO) synthesized by Hummers method, our synthesized GO film, GO-$NH_3$, GO/PIL1-***x***% and GO/PIL1-***x***%-$NH_3$ (***x***= 1 to 5).

| Sample | Strength (MPa) | Strain (%) | Toughness (MJ/m$^3$) | Modulus (GPa) |
|---|---|---|---|---|
| CGO | 103±20 | 2.05±0.54 | 1.34±0.52 | 9.47±1.40 |
| GO | 253±16 | 4.06±0.12 | 5.19±0.43 | 12.06±1.19 |
| GO-$NH_3$ | 242±12 | 1.73±0.31 | 2.55±0.55 | 26.02±1.29 |
| GO/PIL1-1% | 411±42 | 5.38±0.19 | 8.38±1.05 | 11.84±1.75 |
| GO/PIL1-1%-$NH_3$ | 454±57 | 5.77±0.11 | 10.94±1.31 | 14.57±1.78 |
| GO/PIL1-2% | 448±64 | 4.74±0.30 | 9.40±1.76 | 16.28±1.73 |
| GO/PIL1-2%-$NH_3$ | 514±26 | 5.49±0.14 | 12.90±0.62 | 17.40±1.37 |
| GO/PIL1-3% | 511±43 | 5.66±0.21 | 11.41±1.01 | 14.89±1.21 |
| GO/PIL1-3%-$NH_3$ | 585±25 | 5.72±0.22 | 14.93±1.09 | 19.95±2.60 |
| GO/PIL1-4% | 301±46 | 3.69±0.52 | 6.13±1.43 | 14.82±2.13 |
| GO/PIL1-4%-$NH_3$ | 381±22 | 4.47±0.30 | 9.13±0.79 | 17.18±1.27 |
| GO/PIL1-5% | 279±14 | 3.89±0.25 | 5.65±0.56 | 12.64±1.09 |
| GO/PIL1-5%-$NH_3$ | 324±38 | 4.07±0.28 | 7.47±1.24 | 16.73±0.96 |

**Table S4.** The mechanical property data of GO/PIL1-3%-$NH_3$ at different exposure time (0, 3, 15, 24 and 48h) to $NH_3$ vapor.

| GO/PIL1-3%-$NH_3$ | Strength (MPa) | Strain (%) | Toughness (MJ/$m^3$) | Modulus (GPa) |
|---|---|---|---|---|
| 0h | 511±43 | 5.66±0.21 | 11.41±1.01 | 14.89±1.21 |
| 3h | 565±45 | 5.20±0.32 | 11.69±1.52 | 15.93±1.28 |
| 15h | 578±31 | 5.55±0.13 | 12.37±0.65 | 17.33±0.68 |
| 24h | 585±25 | 5.72±0.22 | 14.93±1.09 | 19.95±2.60 |
| 48h | 587±32 | 5.65±0.18 | 12.75±1.10 | 18.18±0.58 |

**Table S5.** The mechanical property data of GO/PIL1-3% and GO/PIL1-3%-$NH_3$ with different thicknesses.

| Sample | Thickness (μm) | Strength (MPa) | Strain (%) | Toughness (MJ/$m^3$) | Modulus (GPa) |
|---|---|---|---|---|---|
| GO/PIL1-3% | 5.53±0.44 | 511±43 | 5.66±0.21 | 11.41±1.01 | 14.89±1.21 |
| GO/PIL1-3%-$NH_3$ | 5.83±0.21 | 585±25 | 5.72±0.22 | 14.93±1.09 | 19.95±2.60 |
| GO/PIL1-3% | 9.81±0.37 | 402±36 | 5.78±0.43 | 11.68±1.47 | 14.76±1.06 |
| GO/PIL1-3%-$NH_3$ | 10.51±0.55 | 527±46 | 5.78±0.56 | 14.27±2.65 | 19.74±0.57 |
| GO/PIL1-3% | 22.56±0.20 | 348±26 | 5.88±0.38 | 9.16±0.82 | 9.33±0.69 |
| GO/PIL1-3%-$NH_3$ | 23.52±0.79 | 465±29 | 6.05±0.59 | 13.98±1.75 | 15.84±1.54 |

**Table S6.** The mechanical property data of control polymer PIL2-based GO nanohybrid films.

| Sample | Strength (MPa) | Strain (%) | Toughness (MJ/m$^3$) | Modulus (GPa) |
|---|---|---|---|---|
| GO/PIL2-1% | 296±14 | 4.00±0.38 | 6.31±1.00 | 10.39±2.04 |
| GO/PIL2-2% | 378±45 | 4.70±0.19 | 7.84±1.08 | 10.98±0.92 |
| GO/PIL2-3% | 496±36 | 4.49±0.31 | 11.27±0.93 | 12.19±3.09 |
| GO/PIL2-3%-$NH_3$ | 478±58 | 4.99±0.36 | 11.32±1.56 | 14.84±1.22 |
| GO/PIL2-4% | 287±22 | 4.44±0.28 | 5.88±0.71 | 12.81±1.01 |
| GO/PIL2-5% | 272±20 | 4.07±0.07 | 5.72±0.89 | 11.35±1.39 |

**Table S7.** The mechanical property data of our GO/PIL1-3%-$NH_3$ film and other GO-based nanohybrid films.

| Materials | Strength (MPa) | Toughness ($MJ/m^3$) | Reference |
|---|---|---|---|
| GO | 253 | 5.0 | In this work |
| GO-$WS_2$-PCDO | 330 | 11.3 | *ACS Nano* **2017**, *11*, 7074 |
| GO-Silk | 300 | 2.4 | *Adv. Mater.* **2013**, *25*, 2301. |
| GO-SF | 153 | 2.6 | *Angew. Chem. Int. Ed.* **2013**, *52*, 13784 |
| *ai*-GO-CNC | 470 | 11.1 | *Adv. Mater.* **2017**, *29*, 1702831. |
| GO-$MoS_2$-TPU | 182 | 5.1 | *ACS Nano* **2015**, *9*, 708 |
| GO-$PAPB_{0.2}$ | 207 | 3.8 | *Adv. Mater.* **2014**, *26*, 7588 |
| GO-CNC-$Cd^{2+}$ | 419 | 11.0 | *Adv. Mater. Interfaces* **2018**, *5*, 1800145 |
| GO-SA | 240 | 1.3 | *Nano Res.* **2016**, *9*, 735 |
| GO-SA-$Nd^{3+}$ | 256 | 4.8 | *Compos. Sci. Technol.* **2017**, *145*, 62 |
| GO-AA-SCMC | 305 | 8.2 | *Adv. Mater.* **2016**, *28*, 2037 |
| GO-CMC-$Al^{3+}$ | 479 | 10.2 | *ACS Nano* **2017**, *11*, 5717 |
| GO-CNC | 490 | 3.9 | *Adv. Mater.* **2016**, *28*, 1501 |
| GO-PDA-Ni | 271 | 4.6 | *Adv. Funct. Mater.* **2017**, *27*, 1605636 |
| GO-MMT-PVA | 331 | 4.9 | *J. Mater. Chem. A* **2015**, *3*, 21194 |
| GO/MMT-CMC | 320 | 7.8 | *Carbohydr. Polym.* **2019**, *222*, 1150262 |
| CMC-SUM-GO | 148 | 4.3 | *ACS Appl. Polym. Mater.* **2019**, *1*, 1505 |
| GO/PDMS−PGMA | 309 | 6.6 | *ACS Appl. Mater. Interfaces* **2016**, *8*, 31264 |
| GO-CMC-$Mn^{2+}$ | 329 | 3.6 | *J. Mater. Chem. A* **2017**, *5*, 16386 |
| GO-DWNT-PCDO | 238 | 4.1 | *ACS Nano* **2015**, *9*, 11568 |

| | | | |
|---|---|---|---|
| TPU/GO-CNTs | 200 | 4.4 | *Compos. Sci. Technol.* **2019**, *179*, 63 |
| GO-CS | 347 | 10.6 | *ACS Nano* **2015**, *9*, 9830 |
| GO-PS | 67 | 3.8 | *RSC Adv.* **2015**, *5*, 28085 |
| GO-SSEBS | 158 | 15.3 | *Carbon* **2017**, *111*, 807. |
| GO-PCDO | 107 | 2.5 | *Angew. Chem. Int. Ed.* **2013**, *52*, 3750 |
| GO-UPy | 326 | 11 | *ACS Nano* **2018**, *12*, 6228 |
| GO-$Al^{3+}$ | 101 | 0.2 | *Nat. Chem.* **2015**, *7*, 166 |
| GO-$Al_2O_3$-PVA | 143 | 9.2 | *ACS Appl. Mater. Interfaces* **2015**, *7*, 9281 |
| GO/SNF/GO | 364 | 12.5 | *ACS Nano* **2020**, *14*, 9701 |
| **GO/PIL1-3%-$NH_3$** | **585** | **14.9** | **In this work** |

**Table S8.** The mechanical property data of pure GO film and the GO/PIL1-3%-$NH_3$ film under different environmental relative humidity.

| Sample | Environmental relative humidity (% RH) | Strength (MPa) | Strain (%) | Toughness ($MJ/m^3$) | Modulus (GPa) |
|---|---|---|---|---|---|
| GO | 20 | 253±16 | 4.06±0.12 | 5.19±0.43 | 12.06±1.19 |
| | 50 | 228±21 | 3.00±0.57 | 3.43±1.03 | 7.17±0.70 |
| | 80 | 226±28 | 3.23±0.58 | 3.71±0.89 | 7.04±1.61 |
| | 98 | 137±32 | 2.25±0.61 | 2.19±1.01 | 4.58±1.42 |
| GO/PIL1-3%-$NH_3$ | 20 | 585±25 | 5.32±0.46 | 14.93±1.09 | 19.95±2.60 |
| | 50 | 527±41 | 5.80±0.47 | 14.72±1.76 | 15.49±3.13 |
| | 80 | 524±44 | 5.19±0.21 | 11.42±1.25 | 14.26±2.07 |
| | 98 | 390±38 | 5.36±0.18 | 7.78±0.75 | 6.86±0.89 |

## Reference

1. X. Lin, X. Shen, Q. Zheng, N. Yousefi, L. Ye, Y.-W. Mai and J.-K. Kim, *ACS Nano*, 2012, **6**, 10708-10719.
2. A. Dimiev, D. V. Kosynkin, L. B. Alemany, P. Chaguine and J. M. Tour, *J. Am. Chem. Soc.*, 2012, **134**, 2815-2822.
3. S. Eigler, S. Grimm, F. Hof and A. Hirsch, *J. Mater. Chem. A*, 2013, **1**, 11559-11562.
4. M. Zhang, Y. Wang, L. Huang, Z. Xu, C. Li and G. Shi, *Adv. Mater.*, 2015, **27**, 6708-6713.